LETTERS

Calcium-bound structure of calpain and its mechanism of inhibition by calpastatin

Rachel A. Hanna[1], Robert L. Campbell[1] & Peter L. Davies[1]

Calpains are non-lysosomal calcium-dependent cysteine proteinases that selectively cleave proteins in response to calcium signals[1] and thereby control cellular functions such as cytoskeletal remodelling, cell cycle progression, gene expression and apoptotic cell death[2–4]. In mammals, the two best-characterized members of the calpain family, calpain 1 and calpain 2 (μ-calpain and m-calpain, respectively), are ubiquitously expressed. The activity of calpains is tightly controlled by the endogenous inhibitor calpastatin, which is an intrinsically unstructured protein capable of reversibly binding and inhibiting four molecules of calpain, but only in the presence of calcium[5,6]. To date, the mechanism of inhibition by calpastatin and the basis for its absolute specificity have remained speculative[7–9]. It was not clear how this unstructured protein inhibits calpains without being cleaved itself, nor was it known how calcium induced changes that facilitated the binding of calpastatin to calpain. Here we report the 2.4-Å-resolution crystal structure of the calcium-bound calpain 2 heterodimer bound by one of the four inhibitory domains of calpastatin. Calpastatin is seen to inhibit calpain by occupying both sides of the active site cleft. Although the inhibitor passes through the active site cleft it escapes cleavage in a novel manner by looping out and around the active site cysteine. The inhibitory domain of calpastatin recognizes multiple lower affinity sites present only in the calcium-bound form of the enzyme, resulting in an interaction that is tight, specific and calcium dependent. This crystal structure, and that of a related complex[10], also reveal the conformational changes that calpain undergoes on binding calcium, which include opening of the active site cleft and movement of the domains relative to each other to produce a more compact enzyme.

The importance of the calpain–calpastatin balance in protection from pathological conditions where calpain is over-activated is well documented. Neurons could be protected from excitotoxic cell death after a glutamate-stimulated rise in intracellular calcium levels, either by overexpression of calpastatin or by expression of a sodium/calcium exchanger that was not cleavable by calpain[11]. In rat hearts subjected to ischaemia/reperfusion injury, overexpression of calpastatin decreased troponin I degradation and contractile dysfunction[12]. These studies benefit from the absolute specificity of calpastatin's inhibition of calpain, something lacking with the widespread use of low molecular weight calpain inhibitors that typically show some inhibition of other cysteine proteases[13].

Calpains 1 and 2 are 100 kDa heterodimers with homologous large subunits comprising four domains (DI–DIV) and a common small subunit with two domains (DV, DVI) (Supplementary Fig. 1). The two carboxy-terminal penta-EF hand (PEF) domains, DIV and DVI, form the major heterodimer interface that holds the two subunits together through the pairing of their fifth EF-hands[14,15]. Each of calpastatin's four inhibitory domains contains three regions of conserved sequence; subdomains A and C bind to DIV and DVI, respectively[16], and subdomain B inhibits calpain via a previously unknown mechanism. As the B subdomain was ineffective at inhibiting the isolated protease core[17] and could be cross-linked to DIII[18], it seemed that the inhibition of the whole enzyme might be allosteric. Others had speculated that the B subdomain might in some way block the active site cleft[8].

To resolve these issues, we co-crystallized the inactive mutant of calpain 2 (C105S)[19] with calpastatin inhibitory domain 4 (CAST4) in the presence of calcium (Supplementary Table 1). The 94-residue CAST4 binds as an extended polypeptide over the surface of calpain, making contact with each domain of the enzyme (Fig. 1, Supplementary Fig. 1) and burying approximately 2,800 $Å^2$ of the surface of calpain (Supplementary Table 2). The calcium-bound structure of calpain is more compact than the apo-form[14,15] because the PEF domains are shifted towards the protease core (DI, DII), decreasing the radius of gyration from 32.2 Å to 30.8 Å (Supplementary Fig. 2). In the process, the amino-terminal anchor helix is displaced from its binding site on the small subunit near EF-hand 1 and is not seen in the electron density, consistent with its tendency to be autoproteolysed during activation of the enzyme.

When bound to calpain, subdomain C forms an amphipathic α-helix that binds to an exposed hydrophobic patch on DVI, just as

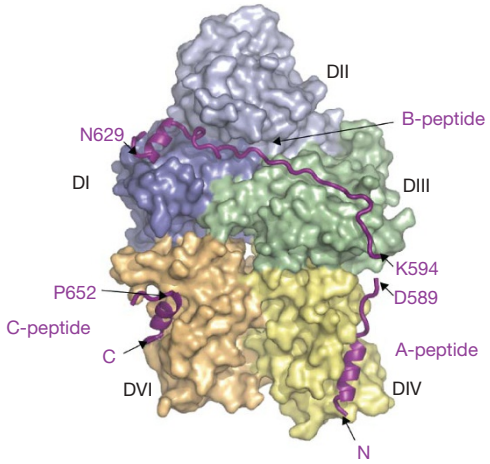

Figure 1 | Overview of calpastatin domain 4 (CAST4) bound to calpain 2. The overall structure of CAST4 (purple) bound to the inactive C105S mutant of calpain 2. CAST4, which is unstructured in the absence of calpain, forms three α-helices when in complex with the enzyme. Helices in subdomains A and C, which are in contact with DIV (yellow) and DVI (orange), and the helix in subdomain B, which is in contact with the protease core DI and DII (blue and light blue, respectively) are shown in ribbon representation. DIII is coloured green. Gaps in the electron density of CAST4 are indicated by missing residues between D589 and K594, and between N629 and P652.

[1]Department of Biochemistry, Queen's University, Kingston, Ontario, Canada K7L 3N6.

©2008 Macmillan Publishers Limited. All rights reserved

previously described[8], and subdomain A forms a similar amphipathic α-helix that interacts with DIV on the large subunit (Supplementary Fig. 3, Supplementary Tables 3 and 4). It is the B subdomain of calpastatin that inhibits calpain[20] while subdomains A and C increase the overall affinity of the interaction. From the crystal structure we see that the B subdomain binds to the activated enzyme on either side of the active site cleft (Fig. 2a, Supplementary Fig. 4, Supplementary Table 5). On the N-terminal side, the inhibitor forms hydrophobic and electrostatic interactions with a shallow groove in DIII (Fig. 2a) that becomes aligned with the catalytic cleft in the holo form of the enzyme. Continuing on into the unprimed side of the cleft, the highly conserved Leu 612 of CAST4 occupies the hydrophobic pocket of the S2 subsite (Fig. 2b, 3b). This leucine is strongly favoured in m-calpain substrates[21], and frequently appears in this position in inhibitors—for example, leupeptin (Fig. 3d). Immediately after Leu 612 the backbone of Gly 613 twists sharply away from the active site and traces the path of what would normally be the side chain of the P1 residue (Fig. 3a, b, Supplementary Fig. 5a, b). In this way, the potentially scissile bond between the P1 and P1′ residues is held ~2 Å out of reach of calpain's catalytic *Cys 105 (asterisk indicates calpain residues) (Fig. 3c). This is demonstrated in our structure, by the proximity of the bond to the *Ser 105 replacement for *Cys 105, which, because this is a calcium-bound structure, is correctly aligned with *His 262 and *Asn 286 of the triad for catalysis.

On the C-terminal side of the B subdomain, calpastatin forms a two-turn amphipathic α-helix that binds to DI (Fig. 2d). Another feature of the C-terminal side of the B subdomain is a seven-residue highly conserved TIPPEYR sequence. The two prolines, Pro 620 and Pro 621, break the helix and redirect CAST4 into the primed side of the cleft while making key contacts with *Trp 288 in DII (Fig. 2c, Supplementary Fig. 6). *Trp 288 is an important residue in the calcium-dependent activation of the protease core, as it reorients from lying across the cleft as a wedge to lining the pocket of the cleft[17]. In particular, the conserved Pro 620 stacks against *Trp 288 and helps pin the C-terminal side of the loop on the primed side of the cleft. Additional hydrophobic contacts come from Ile 619 which projects into the cleft and contacts *Leu 102 and *Ala 101 (Supplementary Fig. 6). Thr 618 (in the TIPPEYR sequence) mirrors Gly 613 by exiting the cleft, oriented such that its side chain projects where the main chain should be, and vice versa (Fig. 2c).

The Leu 612-Gly 613 dipeptide is well conserved across the four inhibitory domains of calpastatin and across a variety of species (Gly 613 is absolutely conserved), as is the TIPPEYR sequence (Supplementary Fig. 7). In between these conserved sequences is a loop out of four typically hydrophilic residues (ERDD) between G and T that are not as well conserved. The KLGE sequence (residues 611–614) forms a type-II β-turn as suggested in ref. 22. The RDDTI sequence (residues 615–619) forms two overlapping, distorted type-I β-turns. For this region to loop out, the flanking portions of the B subdomain (coloured purple and green in Fig. 2a) must each tightly and independently bind to calpain.

This is indeed a novel mechanism. Among proteinaceous inhibitors of proteases, calpastatin is most similar to cystatins that act as a wedge to block the active site and inhibit cathepsins[23]. Cystatins bind as two hairpin loops to both the primed and unprimed side of the active site cleft. Calpastatin is one of only two protease inhibitors that are known to be intrinsically unstructured proteins when not bound to their cognate targets. The other is IA3, an inhibitor of yeast proteinase A, but unlike calpastatin, IA3 is a short (68-residue) polypeptide that is induced to form a nearly perfect helix that blocks the active site of its target[24]. However, in contrast to all other protein inhibitors, calpastatin binds as a contiguous stretch of polypeptide across the complete cleft in such a way that the catalytic cysteine is prevented from reaching the P1 carbonyl. A similar situation exists with the protein phospatase 1–inhibitor 2 (PP1/I-2) complex[25]. Like calpastatin, I-2 is an intrinsically disordered protein that becomes ordered on binding. It also contacts the enzyme in three regions, but is bound in an almost entirely α-helical conformation, unlike calpastatin which maintains a large segment containing no regular secondary structure.

To test our model for the inhibition of calpain by calpastatin, we made three mutations. In the first of these the conserved Gly 613 was

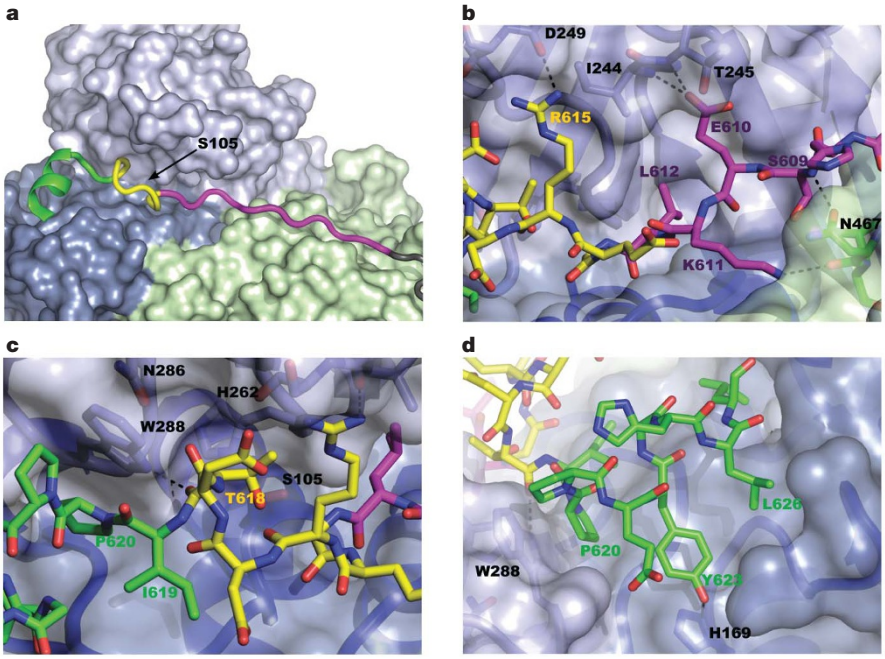

Figure 2 | Specific interactions of calpastatin with calpain entering and leaving the active-site cleft. a–d, The 27-residue B-peptide[7] is coloured as follows: the residues that make the loop out of the active site are coloured yellow, the residues N-terminal to the loop are purple, and the residues C-terminal to the loop are green. Other calpastatin residues are coloured dark grey. Hydrogen-bond interactions of calpastatin with calpain (coloured as in Fig. 1) are shown by black dashed lines. O and N atoms are coloured red and blue, respectively. **a**, Overview of calpain binding at the active site of calpain. **b**, Close-up view of the calpastatin at the unprimed side of the active site. **c**, Close-up view of calpastatin looping away from the catalytic residue. **d**, Close-up view of calpastatin at the primed side of the active site.

©2008 Macmillan Publishers Limited. All rights reserved

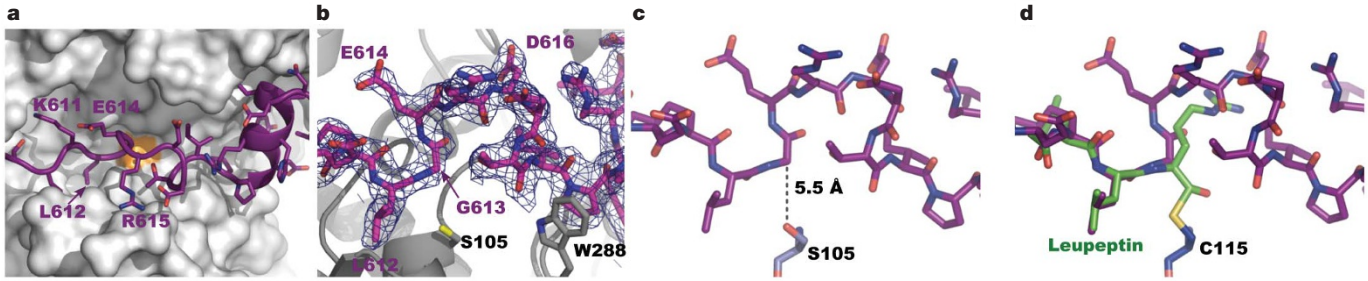

Figure 3 | Close-up views of calpastatin at the active site. a, Representation of calpastatin (purple) looping away from the mutant active-site serine (orange) of calpain (shown uncoloured in space-filling mode). Calpastatin side chains are shown with O atoms in red and N atoms in blue. **b**, Electron density at 1σ for a $2F_o - F_c$ map of the loop region (blue mesh). Calpastatin (purple) backbone O and N atoms are also coloured red and blue, respectively. Calpain (grey) side chains are identified with black lettering. The side chain O atom of *S105 is coloured yellow. **c**, **d**, Comparison of the calpastatin loop region (**c**) with the superimposed leupeptin-bound structure of calpain 1 protease core[28] (**d**). The distance between the active-site serine and the P1 carbonyl of calpastatin is shown by the dotted line (**c**). The structure of leupeptin (green) covalently linked to *Cys115 of calpain 1 is superimposed on the calpastatin loop (**d**) to show how closely the backbone at Gly 613 follows the side chain of the P1 arginine of leupeptin. The P2 leucine of both CAST4 and leupeptin overlap closely.

mutated to Ala to reduce backbone flexibility, rendering CAST4 less able to loop out of the active-site cleft. This single amino acid substitution increased the IC_{50} value 2.9-fold, from 64 to 182 nM (Supplementary Figs 8, 9a). Second, we inserted a Phe residue between Leu 612 and Gly 613 (insert-F) to prevent the formation of the type II β-turn in CAST4 that holds the glycine away from the catalytic cysteine while placing phenylalanine in the P1 position where its peptide bond with glycine should be cleavable. This mutation turned CAST4 from an inhibitor into a substrate. Within a minute of forming the complex, the mutant CAST4 was cut into two fragments of mass 5,068.6 and 5,745.1 Da, which correspond to residues 570–613 and 614–664, respectively (Supplementary Fig. 9b). Interestingly, despite being rapidly cleaved this mutant is still a potent inhibitor of calpain with an IC_{50} of 112 nM, approximately 1.8 times larger than that of the wild type, which makes it a better inhibitor than the G613A mutant (Supplementary Fig. 8). A third mutation, *A101D, was designed to spoil a contact calpastatin makes with the protease core. In calpain 2, *Ala 101 is in a hydrophobic patch that binds calpastatin after the conserved TIPPEYR sequence. *Ala 101 was mutated to aspartic acid to test that we had identified the binding site of subdomain B on calpain. The *A101D mutation caused a 2.2-fold increase in the IC_{50} value of wild-type CAST4 to 146 nM (Supplementary Fig. 8).

In addition to uncovering this mechanism of protease inhibition, the calpastatin–calpain structure reveals for the first time the calcium-bound structure of calpain (Supplementary Fig. 2). The domains have changed little from the calcium-free form. What have changed in the calcium-bound structure of calpain are the relative positions of the domains. In particular, the two PEF domains are closer to the core and have displaced the N-terminal anchor helix. It is not clear to what extent release of the anchor helix helps bring the PEF domains closer to the core and to what extent the domain movement displaces the helix. The overall structural changes are illustrated by a simulation in which Ca^{2+} ions are docked to their binding sites (Supplementary Movie 1). At the 5 mM $CaCl_2$ concentration used for crystallization, four calcium ions are present in both PEF domains. Those in DVI of the small subunit are in exactly the same locations they were in the calcium-bound DVI homodimer structure[8]. Those in DIV of the large subunit are in equivalent locations. Rather surprisingly, despite reports that isolated recombinant DIII can bind Ca^{2+}, there were no calcium ions in contact with this domain in the CAST4-bound structure[26]. The protease core contains the two calcium ions, one in each domain, that are responsible for the cooperative assembly of the catalytic cleft[27]. The arrangement of the core within the whole enzyme is exactly that seen in the crystal structure of the calcium-bound core alone, which validates the mechanism of activation that was elucidated with mutants of the isolated core[27].

By comparing the calpain–calpastatin structure to the calcium-bound structures of the protease core and PEF DVI we see indications that calpastatin recognizes the calcium-bound structure, rather than causing structural changes on binding. As mentioned, subdomains A and C bind when calcium causes a shift in the EF hands, exposing the hydrophobic areas. Without this shift there is not sufficient room for these subdomains to bind[8]. In our structure, the conserved hydrophobic residues of subdomains A and C occupy deep hydrophobic pockets in calpain (Supplementary Fig. 3b, c). Likewise, the structural changes that occur when the protease core binds calcium align the active site, and in particular causes a large change in the position of *Trp 288, without which the B sub-domain could not occupy and bind to the cleft. Also, the rearrangement of the domains relative to one another allows the simultaneous interaction of calpastatin with both DIII and the protease core. This increases the area of interaction, the number of low affinity sites along the length of CAST4, and thus the overall affinity of CAST for calpain. The fact that calpastatin binds only after calpain is activated raises the issue of how closely spaced these proteins are in the cell. Their proximity will probably control the window of opportunity that calpain has for proteolysis during calcium signalling before being inhibited.

The observed shift in DIII is also interesting from the standpoint of designing specific inhibitors to counter the overactivation of calpain that occurs in various diseases[1]. Previous attempts at docking inhibitors have been forced to use the protease core[28], but the structure reported here will enable the design of inhibitors that can take advantage of the complete active site cleft.

METHODS SUMMARY

Inactive calpain 2 with its truncated small subunit (*C105S-m80k/21k) was expressed and purified as previously described[19]. Wild-type CAST4 and the mutants were produced in *Escherichia coli* BL21 (DE3) under kanamycin selection and purified using heat denaturation and HPLC.

To produce the calpain–CAST4 complex, 1 M $CaCl_2$ was added at 6 μl min^{-1} to a mixture of calpain (~15 mg) and a twofold molar excess of CAST4 in 50 ml. The complex was purified using two column chromatography steps: a Ni^{2+}-chelating column (Qiagen), and Superdex 200 C 26/100 column (GE Healthcare). The pure complex was concentrated to 30–40 mg ml^{-1} using an Amicon Ultra-15 30k molecular weight cut-off centrifugal filter (Millipore), aliquoted and flash frozen. The protein solution was added to an equal volume of precipitant solution of 100 mM MES (pH 6.5), 25% PEG 1000 (Qiagen).

Crystallization of the calpain 2 *C105S-m80k/21k–CAST4 complex was performed by the microbatch method under paraffin oil (Hampton). Diffraction data on the calpain–CAST4 complex were collected on a single crystal with approximate dimensions 10 × 50 × 100 μm at the X6A beamline of the NSLS facility (Brookhaven National Laboratory). The structure was determined by molecular replacement using the structure of the calcium-bound protease core[17] and the domains DIII, DIV and DVI of the structure of calcium-free full-length calpain[15].

©2008 Macmillan Publishers Limited. All rights reserved

Full Methods and any associated references are available in the online version of the paper at www.nature.com/nature.

Received 11 March; accepted 24 September 2008.

1. Goll, D. E., Thompson, V. F., Li, H., Wei, W. & Cong, J. The calpain system. *Physiol. Rev.* **83,** 731–801 (2003).
2. Glading, A., Lauffenburger, D. A. & Wells, A. Cutting to the chase: Calpain proteases in cell motility. *Trends Cell Biol.* **12,** 46–54 (2002).
3. Franco, S. J. & Huttenlocher, A. Regulating cell migration: Calpains make the cut. *J. Cell Sci.* **118,** 3829–3838 (2005).
4. Abe, K. & Takeichi, M. NMDA-receptor activation induces calpain-mediated beta-catenin cleavages for triggering gene expression. *Neuron* **53,** 387–397 (2007).
5. Wendt, A., Thompson, V. F. & Goll, D. E. Interaction of calpastatin with calpain: A review. *Biol. Chem.* **385,** 465–472 (2004).
6. Hanna, R. A., Garcia-Diaz, B. E. & Davies, P. L. Calpastatin simultaneously binds four calpains with different kinetic constants. *FEBS Lett.* **581,** 2894–2898 (2007).
7. Betts, R., Weinsheimer, S., Blouse, G. E. & Anagli, J. Structural determinants of the calpain inhibitory activity of calpastatin peptide B27-WT. *J. Biol. Chem.* **278,** 7800–7809 (2003).
8. Todd, B. *et al.* A structural model for the inhibition of calpain by calpastatin: Crystal structures of the native domain VI of calpain and its complexes with calpastatin peptide and a small molecule inhibitor. *J. Mol. Biol.* **328,** 131–146 (2003).
9. Pfizer, J., Assfalg-Machleidt, I., Machleidt, W. & Schaschke, N. Inhibition of human mu-calpain by conformationally constrained calpastatin peptides. *Biol. Chem.* **389,** 83–90 (2008).
10. Moldoveanu, T., Gehring, K. & Green, D. R. Concerted multi-pronged attack by calpastatin to occlude the catalytic cleft of heterodimeric calpains. *Nature* doi:10.1038/nature07353 (this issue).
11. Bano, D. *et al.* Cleavage of the plasma membrane Na^+/Ca^{2+} exchanger in excitotoxicity. *Cell* **120,** 275–285 (2005).
12. Maekawa, A. *et al.* Overexpression of calpastatin by gene transfer prevents troponin I degradation and ameliorates contractile dysfunction in rat hearts subjected to ischemia/reperfusion. *J. Mol. Cell. Cardiol.* **35,** 1277–1284 (2003).
13. Neffe, A. T. & Abell, A. D. Developments in the design and synthesis of calpain inhibitors. *Curr. Opin. Drug Discov. Dev.* **8,** 684–700 (2005).
14. Hosfield, C. M., Elce, J. S., Davies, P. L. & Jia, Z. Crystal structure of calpain reveals the structural basis for Ca(2+)-dependent protease activity and a novel mode of enzyme activation. *EMBO J.* **18,** 6880–6889 (1999).
15. Strobl, S. *et al.* The crystal structure of calcium-free human m-calpain suggests an electrostatic switch mechanism for activation by calcium. *Proc. Natl Acad. Sci. USA* **97,** 588–592 (2000).
16. Takano, E., Ma, H., Yang, H. Q., Maki, M. & Hatanaka, M. Preference of calcium-dependent interactions between calmodulin-like domains of calpain and calpastatin subdomains. *FEBS Lett.* **362,** 93–97 (1995).
17. Moldoveanu, T. *et al.* A Ca(2+) switch aligns the active site of calpain. *Cell* **108,** 649–660 (2002).
18. Croall, D. E. & McGrody, K. S. Domain structure of calpain: Mapping the binding site for calpastatin. *Biochemistry* **33,** 13223–13230 (1994).
19. Elce, J. S., Hegadorn, C., Gauthier, S., Vince, J. W. & Davies, P. L. Recombinant calpain II: Improved expression systems and production of a C105A active-site mutant for crystallography. *Protein Eng.* **8,** 843–848 (1995).
20. Maki, M. *et al.* Inhibition of calpain by a synthetic oligopeptide corresponding to an exon of the human calpastatin gene. *J. Biol. Chem.* **264,** 18866–18869 (1989).
21. Cuerrier, D., Moldoveanu, T. & Davies, P. L. Determination of peptide substrate specificity for mu-calpain by a peptide library-based approach: The importance of primed side interactions. *J. Biol. Chem.* **280,** 40632–40641 (2005).
22. Ishima, R. *et al.* Structure of the active 27-residue fragment of human calpastatin. *FEBS Lett.* **294,** 64–66 (1991).
23. Otlewski, J., Filip, J., Zakrzewska, M. & Oleksy, A. The many faces of protease-protein inhibitor interaction. *EMBO J.* **24,** 1304–1310 (2005).
24. Li, M. *et al.* The aspartic proteinase from *Saccharomyces cerevisiae* folds its own inhibitor into a helix. *Nature Struct. Biol.* **7,** 113–117 (2000).
25. Hurley, T. D. *et al.* Structural basis for regulation of protein phosphatase 1 by inhibitor-2. *J. Biol. Chem.* **282,** 28874–28883 (2007).
26. Tompa, P., Emori, Y., Sorimachi, H., Suzuki, K. & Friedrich, P. Domain III of calpain is a Ca^{2+}-regulated phospholipid-binding domain. *Biochem. Biophys. Res. Commun.* **280,** 1333–1339 (2001).
27. Moldoveanu, T., Jia, Z. & Davies, P. L. Calpain activation by cooperative Ca^{2+} binding at two non-EF-hand sites. *J. Biol. Chem.* **279,** 6106–6114 (2004).
28. Moldoveanu, T., Campbell, R. L., Cuerrier, D. & Davies, P. L. Crystal structures of calpain-E64 and -leupeptin inhibitor complexes reveal mobile loops gating the active site. *J. Mol. Biol.* **343,** 1313–1326 (2004).

Supplementary Information is linked to the online version of the paper at www.nature.com/nature.

Acknowledgements This work was funded by the Canadian Institutes for Health Research. R.A.H. is the recipient of a Bauman Fellowship and an R.J. Wilson Fellowship. P.L.D. holds a Canada Research Chair in Protein Engineering. We are grateful to S. Gauthier for technical assistance, to M. Kuiper for the simulation of the conformational change in calpain on binding Ca^{2+}, to the Queen's University Protein Function Discovery (PFD) Facility and D. McLeod for mass spectrometry, Z. Jia for access to data collection on a home source and to M. Allaire at Brookhaven National Laboratory for assistance with data collection on beam line X6A.

Author Information Structure factors and coordinates have been deposited in the RCSB Protein Data Bank with the accession number 3BOW. Reprints and permissions information is available at www.nature.com/reprints. Correspondence and requests for materials should be addressed to P.L.D. (peter.davies@queensu.ca).

©2008 Macmillan Publishers Limited. All rights reserved

METHODS

Data analysis and structure solution. The oscillation data were processed using HKL2000[29] and the CCP4 software suite[30]. The structure was determined by molecular replacement using the automated search method of phaser[31,32]. The structure was refined with refmac5 using the TLS protocol[33].

Kinetic analysis. Calpain assays of the hydrolysis of a FRET-linked peptide substrate were performed in triplicate in a final volume of 1 ml. The concentrations of inhibitors ranged from 24 nM to 2.2 μM. The concentration of wild-type and mutant calpain 2 was 50 nM. The end-point fluorescence intensity was measured in a LS 50B fluorimeter (Perkin Elmer). The IC_{50} values were obtained by three-parameter sigmoidal fitting using the data graphing software SigmaPlot (Systat Software Inc.). Calpain was mixed with varying concentrations of CAST in 500 μl of 50 mM HEPES-HCl (pH 7.4). Reactions were initiated by the addition of 500 μl of 50 mM HEPES-HCl (pH 7.4), 2 mM $CaCl_2$, 2 mM DTT, and 10 μM (EDANS)-EPLFAERK-(DABCYL), the fluorogenic substrate of calpain[21]. The reaction was allowed to proceed for 20 min and was stopped with 10 μl of 0.5 M EDTA. Fluorescence intensity was measured using wavelengths of 335 nm for excitation and 505 nm for emission.

Limited proteolysis and identification of cleavage products of the insert-F mutant. Proteolytic digestion of the CAST4 insert-F mutant (40 nM) by calpain 2 (400 nM) was performed at 22 °C in 10 mM HEPES-HCl (pH 7.4), 1 mM dithiothreitol in 200 μl total volume. Digestion was initiated by the addition of $CaCl_2$ to a concentration of 1 mM and was stopped at 1 min by the addition of EDTA to a concentration of 100 mM. Digestion of the insert-F mutant was accessed by 10% SDS–PAGE and Coomassie blue staining. The insert-F fragments were excised from the gel, and digestion analysis by MALDI-TOF mass spectrometry was performed at the Protein Function Discovery facility (Queen's University, Kingston, Canada).

29. Minor, W., Cymborowski, M., Otwinowski, Z. & Chruszcz, M. HKL-3000: The integration of data reduction and structure solution — from diffraction images to an initial model in minutes. *Acta Crystallogr. D* **62**, 859–866 (2006).
30. Collaborative Computational Project Number 4. The CCP4 suite: Programs for protein crystallography. *Acta Crystallogr. D* **50**, 760–763 (1994).
31. Read, R. J. Pushing the boundaries of molecular replacement with maximum likelihood. *Acta Crystallogr. D* **57**, 1373–1382 (2001).
32. Storoni, L. C., McCoy, A. J. & Read, R. J. Likelihood-enhanced fast rotation functions. *Acta Crystallogr. D* **60**, 432–438 (2004).
33. Winn, M., Isupov, M. & Murshudov, G. N. Use of TLS parameters to model anisotropic displacements in macromolecular refinement. *Acta Crystallogr. D* **57**, 122–133 (2001).

©2008 Macmillan Publishers Limited. All rights reserved